Optimization Under Uncertainty of Nonlinear Energy Sinks

Ethan Boroson, Samy Missoum, Pierre-Olivier Mattei, Christophe Vergez

OPTIMIZATION UNDER UNCERTAINTY OF NONLINEAR ENERGY SINKS

Ethan Boroson
Computational Optimal Design of Engineering Systems (CODES) Laboratory
Department of Aerospace and Mechanical Engineering
University of Arizona
Tucson, Arizona 85721
Email: ethanboroson@email.arizona.edu

Samy Missoum*
Computational Optimal Design of Engineering Systems (CODES) Laboratory
Department of Aerospace and Mechanical Engineering
University of Arizona
Tucson, Arizona 85721
Email: smissoum@email.arizona.edu

Pierre-Olivier Mattei
Laboratoire de Mécanique et d'Acoustique (LMA)
CNRS, UPR 7051
Aix-Marseille University, Centrale Marseille
Marseille 13402, France
Email: mattei@lma.cnrs-mrs.fr

Christophe Vergez
Laboratoire de Mécanique et d'Acoustique (LMA)
CNRS, UPR 7051
Aix-Marseille University, Centrale Marseille
Marseille 13402, France
Email: vergez@lma.cnrs-mrs.fr

ABSTRACT

Nonlinear Energy Sinks (NES) are used to passively reduce the amplitude of vibrations. This reduction is made possible by introducing a nonlinearly stiffening behavior in the NES, which might lead to an irreversible transfer of energy between the main system (e.g., a building) and the NES. However, this irreversible transfer, and therefore the efficiency of the NES, is strongly dependent on the design parameters of the NES. In fact, the efficiency of the NES might be so sensitive to changes in design parameters and other factors (e.g., initial conditions) that it is discontinuous, switching from efficiency to inefficiency for a small perturbation of parameters. For this reason, this work introduces a novel technique for the optimization under uncertainty of NES. The approach is based on a support vector machine classifier, which is insensitive to discontinuities and allows one to efficiently propagate uncertainties. This enables one to efficiently solve an optimization under uncertainty problem. The various techniques presented in this paper are applied to an analytical NES example.

1 INTRODUCTION

Nonlinear Energy Sinks (NES) have become a promising approach for the reduction of vibrations [1]. They have several high-impact applications in fields such as earthquake engineering [2, 3] and aeroelasticity [4]. NESs are particularly attractive because they are passive, thus offering a higher level of reliability than active systems. In addition, NESs are more robust and efficient than traditional tuned mass damper (TMD) systems and work over a larger frequency range [3].

A NES is coupled to a main system (e.g., a building), for which one wants to reduce the amplitude when subjected to a transient loading. The reduction of amplitude is achieved by an irreversible flow of energy between the main system and the NES which "captures and dissipates" this energy. This irreversibility is made possible because of the nonlinear stiffness property of the NES [1].

*Address all correspondence to this author.

However, irreversibility and efficiency are dictated by the NES design parameters which need to be optimally selected. It has also been realized that uncertainties might play an important role in the behavior and efficiency of the NES and several uncertainty quantification techniques such as polynomial chaos expansions have been used [5].

In this work, it is first shown that accounting for uncertainties is essential in the design of NES because the efficiency of a NES might be discontinuous. In fact, the discontinuities might be so marked that the NES can switch from a "high" to a "low" efficiency for a slight perturbation of design parameters or initial conditions. This observation implies that a specific design optimization method is needed since techniques such as gradient-based methods would be inadequate or would lead to a non-robust design.

This paper proposes an optimization under uncertainty method which starts by explicitly identifying the regions of the design space where an "acceptable" NES efficiency is obtained. The boundaries of this region are obtained using a support vector machine (SVM) classifier which is trained using a dedicated adaptive sampling scheme. This approach, whereby regions of the space, even disjoint and non-convex, are identified, is referred to as explicit design space decomposition (EDSD). The use of a classification technique such as SVM makes the approach insensitive to discontinuities and enables one to segregate NES designs that are efficient and inefficient. Another important aspect of this work is that NESs are not classified as efficient or inefficient based on an *a priori* threshold of a given metric (e.g., decay) but are differentiated through an unsupervised clustering technique such as K-means, which, in essence, detects the discontinuities. Once the SVM boundary is constructed, the probability of belonging to the low-efficiency region can be calculated for any point in the parameter space using the SVM as a limit state. Subsequently, a reliability-based design optimization (RBDO) problem can be solved.

In order to quantify the efficiency of the NES, two metrics are used. The first one is the fraction of energy dissipated by the NES [6]. However, this metric alone might not, *a priori*, be enough to measure how efficient the NES is. For this reason, a second metric quantifies the time needed to reach the corresponding amount of dissipated energy.

This paper will first provide an introduction to NES and demonstrate the presence of an efficiency discontinuity. The construction of SVM based on clustering and adaptive sampling is then presented. This is followed by a description of the calculation of probabilities of failure as well as the RBDO methodology. These steps will be demonstrated on a simple analytical two DOF system. Of particular importance, the optimization will show that it is possible to design a NES so as to maximize its efficiency while accounting for uncertainties.

1.1 Example of NES: 2 DOF System

A simple two DOF system can be used to illustrate the basic principle of NES [6] and is depicted in Figure 1. It is composed of a main system 1 (with angular eigen-frequency ω_1, damping λ_1) and a sub-system 2 (the NES)

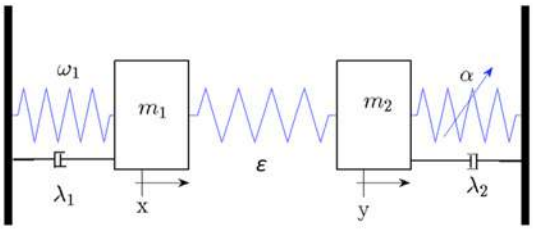

FIGURE 1. Example of 2 DOF system with NES

$$\begin{cases} \ddot{x} + \lambda_1 \dot{x} + \omega_1^2 x + \varepsilon(x-y) = 0 \\ \ddot{y} + \lambda_2 \dot{y} + \alpha y^3 + \varepsilon(y-x) = 0 \end{cases} \tag{1}$$

where ε is used to couple the main system and the NES. The NES is characterized by a nonlinear (cubic) stiffness term with coefficient α which is necessary for the energy pumping mechanism. Figure 2 depicts a case with irreversible energy transfer where the NES proves to be efficient in reducing the oscillation amplitude of the main system. Without the nonlinearity, there would be, in general, an exchange of energy between the two systems.

1.2 Efficiency metrics

In this article, two efficiency metrics are used to characterize the NES. The first one is the asymptotic value of the ratio of dissipated energy to the initial kinetic energy:

$$E_{NES_{inf}} = \lim_{t \to \infty} E_{NES}(t) \tag{2}$$

where

$$E_{NES}(t) = \frac{\lambda_2 \int_0^t \dot{y}(\tau)^2 d\tau}{\frac{1}{2}\dot{x}_0^2} \tag{3}$$

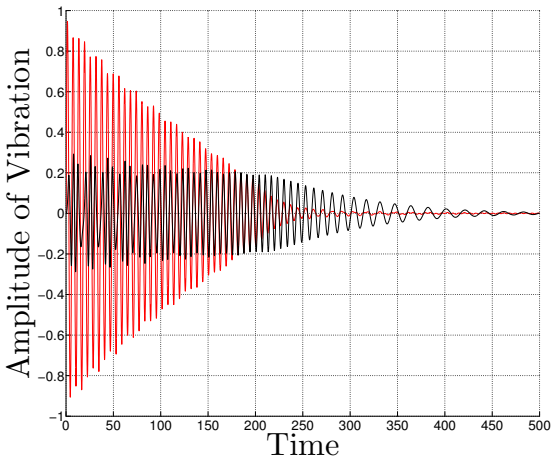

FIGURE 2. Example of irreversible transfer of energy to the NES leading to an efficient reduction of amplitude of the main system.

where $\dot{x}_0 = \dot{x}(0)$ is the (imposed) initial velocity of the main system.

However, this metric alone might not be sufficient, as it does not provide information about how fast the energy is dissipated. For this reason, the time for the main system to reach 99% of its initial energy is also computed:

$$t_{99} = t^* / \frac{\frac{1}{2}(k_1 x^2(t^*) + m_1 \dot{x}^2(t^*))}{\frac{1}{2} m_1 \dot{x}_0^2} = 0.01 \tag{4}$$

Dividing by m_1:

$$t_{99} = t^* / \frac{\omega_1^2 x^2(t^*) + \dot{x}^2(t^*)}{\dot{x}_0^2} = 0.01 \tag{5}$$

1.3 Discontinuity of NES efficiency metrics

The design of NES could be thought to be possible through well-established design optimization methods. However, it has been observed that the NES efficiency is very sensitive to uncertainties. In fact, it is so sensitive that it exhibits a discontinuous behavior. An example of a marked discontinuity is depicted in Figure 4 which depicts the t_{99} metric for a number of α, ε values. The clusters resulting from the discontinuity can be identified using a clustering technique such as K-means [7] which is instrumental in the proposed optimization approach. It is noteworthy that this technique does not require an *a priori* knowledge about where the discontinuity appears. The same type of behavior is obtained when using the $E_{NES_{inf}}$ metric (Figure 5).

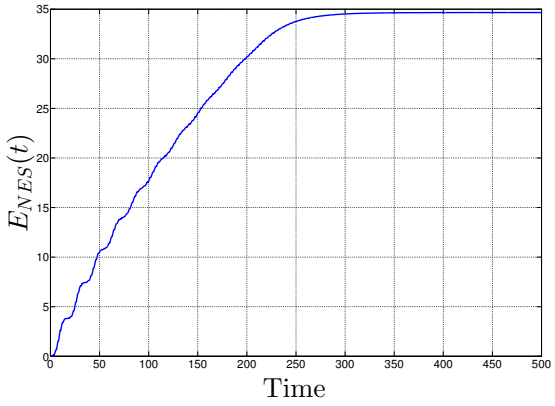

FIGURE 3. Example plot of $E_{NES}(t)$. $E_{NES_{inf}}$ is the final $E_{NES}(t)$ value.

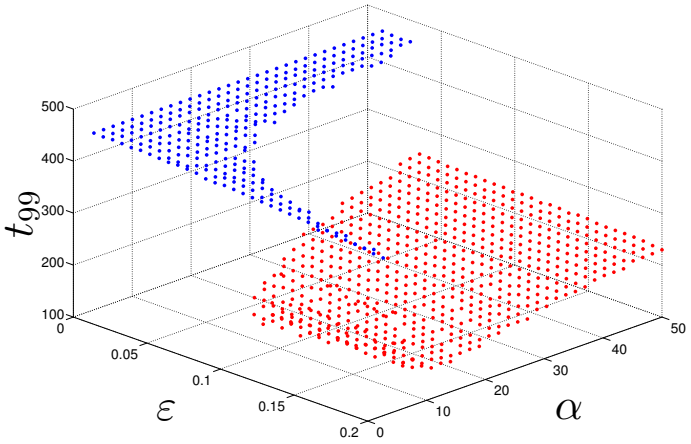

FIGURE 4. Example of discontinuity in NES efficiency as measured by the t_{99} metric. Two clusters are formed (red and blue) and can be identified without *a priori* knowledge using a clustering technique.

For the experiments perfromed by the authors, it is noteworthy that both metrics seem to exhibit discontinuities for the same α, ε configurations. Therefore, either metric could be used to define the failure region. However, from a computational standpoint, the time metric typically offers more separated clusters than the energy metric and therefore allows for a more straightforward identification of the regions. This can be observed from Figure 6. Note that, the fact that the clusters are more clearly defined for t_{99} might not be general and seem to happen for cases where $\lambda_1 < \lambda_2$.

2 CONSTRUCTION OF FEASIBLE REGIONS USING SVM

Beyond clustering of the system's responses, we would like to identify the region of the parameter space where the efficiency

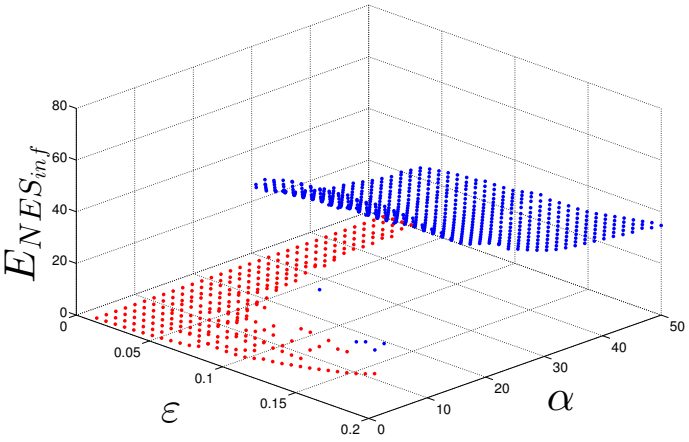

FIGURE 5. Example of discontinuity in NES efficiency as measured by the $E_{NES_{inf}}$ metric. Two clusters are formed (red and blue) and can be identified without *a priori* knowledge using a clustering technique.

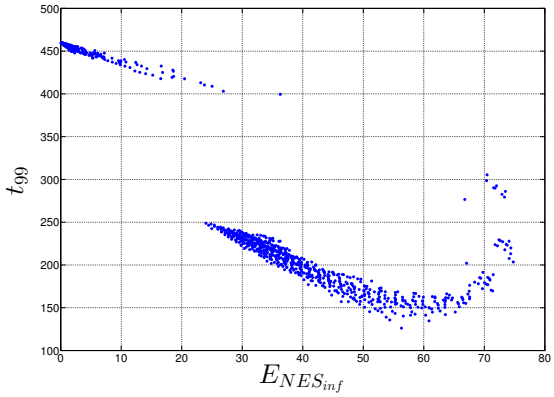

FIGURE 6. Example of $E_{NES_{inf}}$ values and t_{99} values. The separation between two clusters is clearer for t_{99}.

of the NES is "acceptable". In other words, we would like to find the region of the space corresponding to the cluster of better efficiency, either using the t_{99} or the $E_{NES_{inf}}$ metric. For this purpose, we will use a technique referred to as explicit design space decomposition (EDSD) [8, 9]. The basic idea is to construct the boundary separating two classes of samples (e.g., belonging to the two clusters) in terms of chosen parameters. This is achieved using a Support Vector Machine (SVM) [10, 11] which provides an explicit expression of the boundary in terms of the parameters.

2.1 Support Vector Machines (SVMs)

SVM is a machine learning technique widely used for classification. In reliability assessment, SVMs are used to approximate highly nonlinear constraints and limit-state functions. The two most important features of SVMs are their ability to handle multiple failure modes using a single classifier and their insensitivity to discontinuities [12].

An SVM defines an explicit boundary that separates samples belonging to two classes labeled as $+1$ and -1. Given a set of N training samples $\mathbf{x}_i$ in an n-dimensional space and the corresponding class labels y_i, an SVM boundary is given as:

$$s(\mathbf{x}) = b + \sum_{i=1}^{N} \lambda_i y_i K(\mathbf{x_i}, \mathbf{x}) = \mathbf{0} \tag{6}$$

where b is a scalar referred to as the bias, λ_i are Lagrange multipliers obtained from the quadratic programming optimization problem used to construct the SVM, and K is a kernel function. The classification of any arbitrary point $\mathbf{x}$ is given by the sign of $s(\mathbf{x})$. The training samples for which the Lagrange multipliers are non-zero are referred to as the *support vectors*. The kernel function K in Equation 6 can have several forms, such as polynomial or Gaussian radial basis kernel. The Gaussian kernel (Equation 7) is used in this article.

$$K(\mathbf{x}_i, \mathbf{x}_j) = \exp\left(-\frac{||\mathbf{x}_i - \mathbf{x}_j||^2}{2\sigma^2}\right) \tag{7}$$

where σ is the width parameter.

In the case of NES, the classes of the samples are defined using the clusters to which they have been assigned. However, this is not the only choice and the classes can also be defined using a specific, user-defined, threshold. An initial approximation of the SVM boundary is obtained using a design of experiments (DOE) [13, 14] such as Latin Hypercube Sampling (LHS) or Central Voronoi Tessellation (CVT). The boundary is then refined using an adaptive sampling scheme as described below.

2.2 Refinement of the SVM boundary. Adaptive sampling.

The adaptive sampling scheme is described in detail in [8]. A fundamental aspect of the algorithm is the selection of samples in the sparse regions of the space (i.e., as far away as possible from existing samples) and also in the regions of highest probability of misclassification by the SVM. The latter criterion is obtained by locating the samples on the SVM. These samples are found by solving the following global optimization problem:

$$\begin{aligned} \max_{\mathbf{x}} \quad & ||\mathbf{x} - \mathbf{x}_{nearest}|| \\ s.t. \quad & s(\mathbf{x}) = 0 \end{aligned} \tag{8}$$

Figure 7 depicts an example of boundary constructions for the 2 DOF NES. The results section will provide examples of

three dimensional boundaries constructed using both design and aleatory variables.

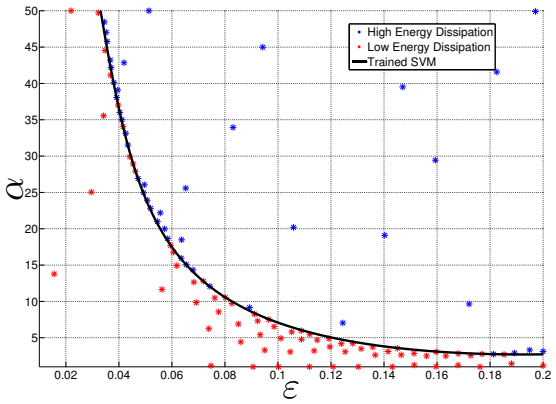

FIGURE 7. Boundary separating the two levels of NES efficiency identified through clustering of $E_{NES_{inf}}$. Construction based on adaptive sampling.

3 PROBABILITY ESTIMATES

Once an SVM boundary is constructed, the probability that a configuration belongs to a specific class (e.g., belongs to the region of low NES efficiency) can be very efficiently obtained through Monte-Carlo simulations [15]. Given the probability density functions of the parameters, the probability P_f of belonging to the "positive" class is approximated using N_{MC} samples $\mathbf{p}_i$:

$$P_f = \frac{1}{N_{MC}} \sum_{i=1}^{N_{MC}} I_s(\mathbf{p}_i), \tag{9}$$

where I_s is the indicator function defined as:

$$I_s = \begin{cases} 0 & \text{if } s(\mathbf{p}_i) \leq 0 \\ 1 & \text{if } s(\mathbf{p}_i) > 0 \end{cases}$$

As an example, consider the two DOF system for which the parameters α and ε are considered uncertain with normal distributions. For various values of the means of α and ε, the probability of belonging to the high efficiency NES region as defined by clustering and SVM (Figure 7)is determined. 10^5 Monte-Carlo samples are used.

4 RELIABILITY-BASED DESIGN OPTIMIZATION

The efficient calculation of probabilities with SVM using Monte-Carlo simulations can be used towards the solution of a reliability-based design optimization (RBDO) problem [12], which in the case of a NES, could be formulated as follows:

$$\max_{\mu^{\mathbf{d}}} \quad \mathbb{E}(E_{NES_{inf}}(\mathbf{X^d}, \mathbf{X^a})) \tag{10}$$

$$s.t. \quad \mathbb{P}((\mathbf{X^d}, \mathbf{X^a}) \in \Omega) \leq P_T$$
$$\mu^{\mathbf{d}}_{\mathbf{min}} \leq \mu^{\mathbf{d}} \leq \mu^{\mathbf{d}}_{\mathbf{max}} \tag{11}$$

where $\mathbb{E}$ is the expected value, $\mu^{\mathbf{d}}$ is the vector of hyper-parameters of the distributions of the random design variables $\mathbf{X}^d$. $\mathbf{X}^a$ are aleatory random variables which contribute to the expected value of the objective function as well as the probabilistic constraints, but whose hyper-parameters are not to be optimized. A typical choice of hyper-parameters to optimize are the means of the normal distributions. Ω is the failure region as defined by the SVM boundary, P_T is a target probability.

Note that the probabilistic constraint in the previous problem cannot be used as such because of the noise introduced by the Monte-Carlo simulations which would make the constraint non-differentiable. For this reason, this constraint is typically approximated using a response surface or a metamodel such as Kriging. To regularize the problem further the reliability index β is approximated instead of the probability P_f itself [12]. β can be defined using the standard cumulative distribution function Φ:

$$\beta = -\Phi^{-1}(P_f) \tag{12}$$

To further reduce computational time and make this RBDO problem tractable, the objective function is also approximated using a metamodel such as Kriging.

4.1 APPLICATION TO THE 2 DOF SYSTEM

Two RBDO problems are solved for the 2 DOF system depicted in Figure 1. The first RBDO problem is two-dimensional and only contains random design variables. The second one adds the initial velocity of the main system $\dot{x}_0$ as an aleatory variable. In both cases, the failure domain Ω is defined by the SVM constructed from the time metric (see Section 1.3). Throughout the results section, the default values of parameters not used in the optimizations are: $\omega_1 = 1.0$; $\lambda_1 = 0.01$; $\lambda_2 = 0.03$; $\dot{x}_0 = 1$.

4.1.1 Problem I. Two-dimensional problem.

$$\max_{\mu_\alpha,\mu_\varepsilon} \quad \mathbb{E}(E_{NES_{inf}}(\mu_\alpha,\mu_\varepsilon)) \tag{13}$$

$$s.t. \quad \mathbb{P}((\alpha,\varepsilon)\in\Omega) \le 10^{-2}$$
$$1.0 \le \mu_\alpha \le 50$$
$$0.01 \le \mu_\varepsilon \le 0.2 \tag{14}$$

where α and ε follow normal distributions: $\alpha \sim N(\mu_\alpha, 4.9^2)$ and $\varepsilon \sim N(\mu_\varepsilon, 0.019^2)$.

In order to have a better understanding of the problem, $E_{NES_{inf}}$ is plotted over the whole search space (ε, α) (Figure 8). The plot clearly shows that an unconstrained deterministic optimization of the energy might lead to a non-robust design. In fact, with the random distributions provided, this design would have a 10% probability of "switching" to the other side of the discontinuity where efficiency is low. Therefore, the problem is constrained by the SVM-defined failure region (Figure 9) constructed using adaptive sampling. From this SVM, the probability of being in the failure space is depicted in Figure 10 through the reliability index β. The optimal result is depicted in Figure 11 and is summarized in Table 1. At the optimum, the (approximated) probabilistic constraint is active. The actual probability of failure, as calculated based on the SVM is also provided in the table.

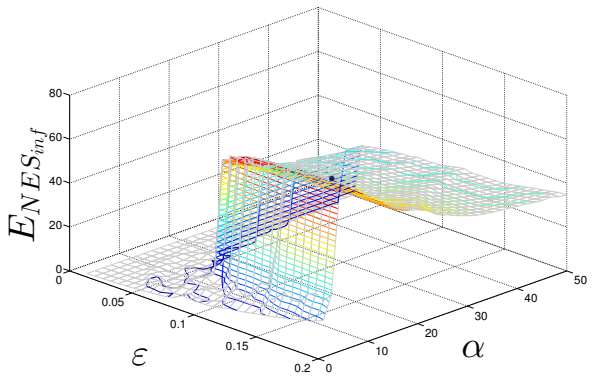

FIGURE 8. $E_{NES_{inf}}$ as a function of α and ε (initial velocity of the main system $\dot{x}_0$=1). The deterministic optimum is shown (blue dot). A small perturbation in design parameters from this optimum could result in an inefficient NES.

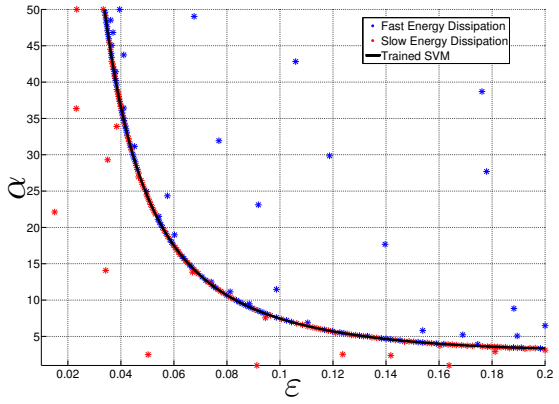

FIGURE 9. Boundary separating the two levels of NES efficiency identified through clustering on t_{99}. Construction based on adaptive sampling.

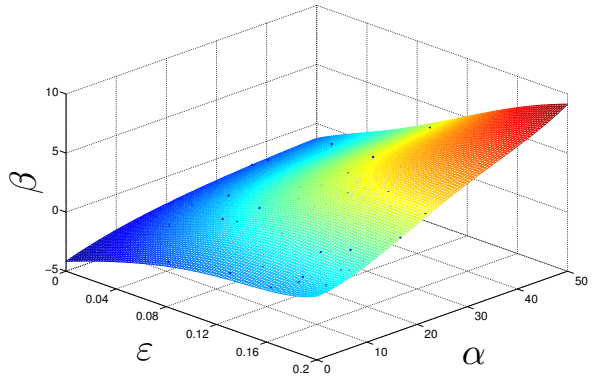

FIGURE 10. Training points and Kriging approximation of β values for the two dimensional RBDO problem.

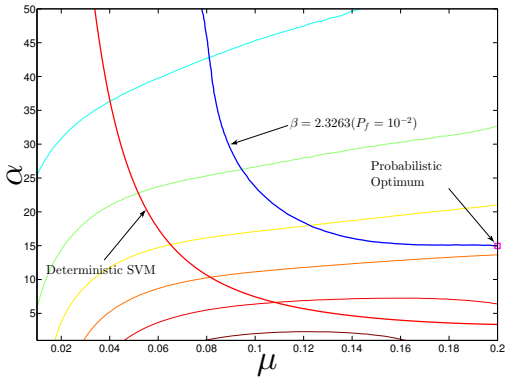

FIGURE 11. Results of the optimization. 2D RBDO problem.

4.1.2 Problem II. Three-dimensional problem with aleatory variable.

The second optimization problem involves random design variables as well as a purely aleatory variable $\dot{x}_0$ (initial velocity of the main system) with uniform distri-

TABLE 1. Results of 2D RBDO problem.

	Probabilistic Optimum
ε	0.20
α	14.95
Actual P_f	0.0090
$\tilde{\mathbb{E}}(\tilde{E}_{NES_{inf}})^*$	58.27 %
$\mathbb{E}(\tilde{E}_{NES_{inf}})^\dagger$	58.13 %

* Approximated $\mathbb{E}$ and $E_{NES_{inf}}$
† Approximated $E_{NES_{inf}}$

bution $\dot{x}_0 \sim U(0.25, 1)$.

$$\max_{\mu_\alpha, \mu_\varepsilon} \quad \mathbb{E}(E_{NES_{inf}}(\mu_\alpha, \mu_\varepsilon, \dot{x}_0)) \tag{15}$$

$$s.t. \quad \mathbb{P}((\alpha, \varepsilon, \dot{x}_0) \in \Omega) \leq 5 * 10^{-2}$$

$$1 \leq \mu_\alpha \leq 50$$

$$0.01 \leq \mu_\varepsilon \leq 0.2 \tag{16}$$

$$\tag{17}$$

As mentioned in Section 1.3, the probabilistic constraint is better handled, at least for the present study, by using the time metric instead of the energy metric. This can be better understood by investigating the SVM for the energy (Figure 12) and the time (Figure 13). Indeed, both share the same discontinuous behaviors in the same regions of the space but a slightly different SVM is obtained. This difference stems from the clustering, which in the case of the energy, (Figure 14) is not as well separated as for the time metric (Figure 15). In other words, the clustering for the energy does not solely isolate the discontinuities.

Figure 16 depicts the approximation of β. Optimization results are depicted in Figure 17 and listed in Table 2. The probabilistic constraint is active and the actual probability of failure calculated based on the SVM is 5.1%, slightly violating the target probability.

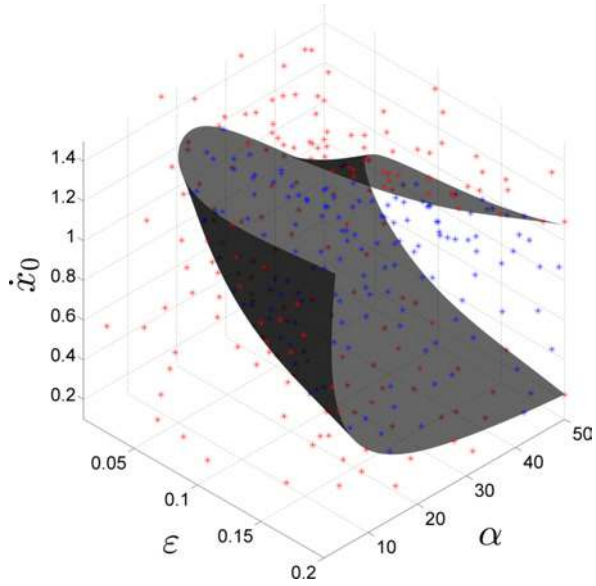

FIGURE 12. Three dimensional boundary separating the two levels of NES efficiency identified through clustering of $E_{NES_{inf}}$. Parameters: α, ε, and initial velocity of the main system $\dot{x}_0$.

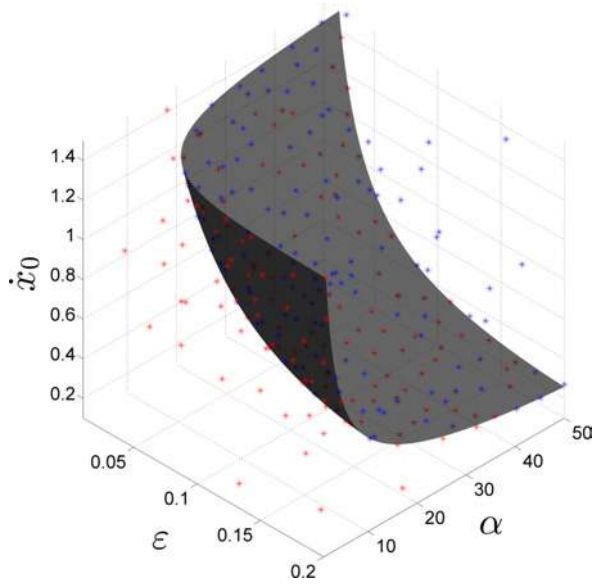

FIGURE 13. Three dimensional boundary separating the two levels of NES efficiency identified through clustering of t_{99}. Parameters: α, ε, and initial velocity of the main system $\dot{x}_0$.

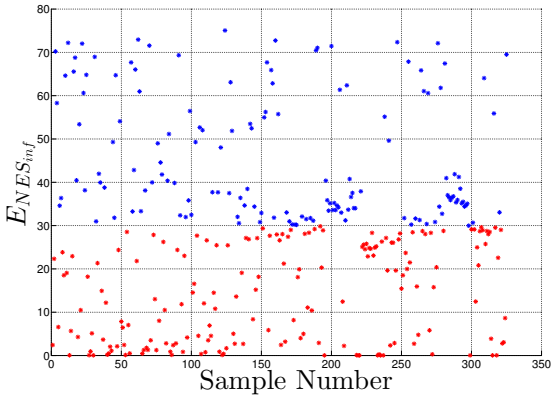

FIGURE 14. K-means clustered values of $E_{NES_{inf}}$ with varied α, ε and $\dot{x}_0$. The clusters are not well separated, due to the nature of $E_{NES_{inf}}$.

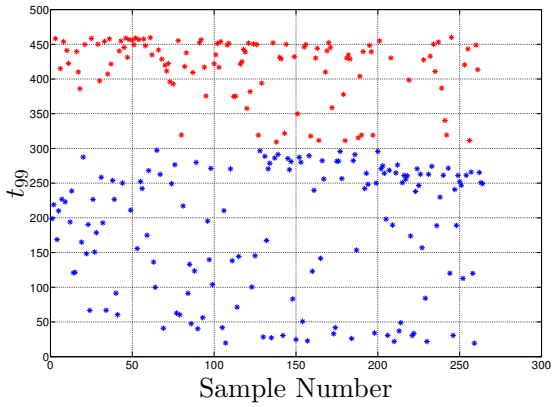

FIGURE 15. K-means clustered values of t_{99} with varied α, ε and $\dot{x}_0$. The clusters are more separated than those of $E_{NES_{inf}}$.

TABLE 2. Results of 3D RBDO problem.

	Probabilistic Optimum
ε	0.1999
α	39.4968
Actual P_f	0.0510
$\tilde{\mathbb{E}}(\tilde{E}_{NES_{inf}})^*$	57.9206 %
$\mathbb{E}(\tilde{E}_{NES_{inf}})^\dagger$	57.9391 %

* Approximated $\mathbb{E}$ and $E_{NES_{inf}}$

† Approximated $E_{NES_{inf}}$

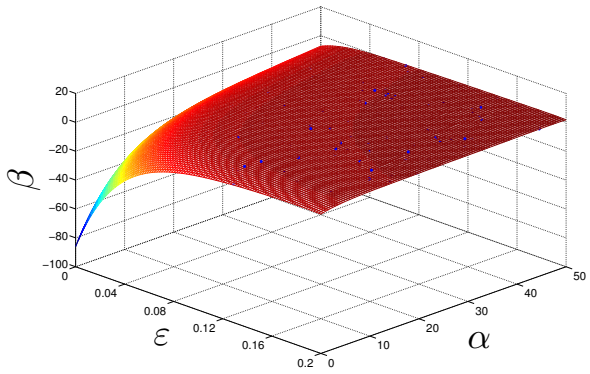

FIGURE 16. Training points and Kriging approximation of β for the 3 dimensional RBDO case.

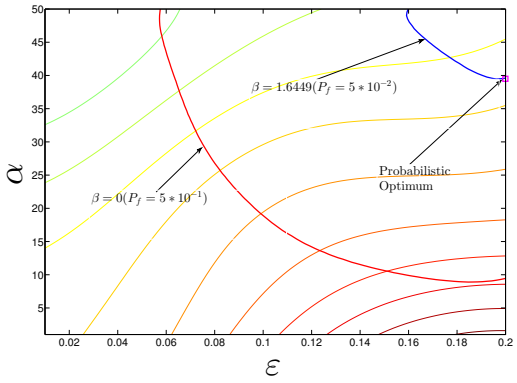

FIGURE 17. Results of the 3D RBDO Problem. Probabilistic optimum shown with iso-contours of β and Kriging approximation of $\mathbb{E}(E_{NES_{inf}})$.

5 CONCLUSION

This paper introduces a new methodology for the optimization under uncertainty of NES. The methodology stems from the realization that the efficiency of a NES might be discontinuous and highly sensitive to uncertainty. For this reason, specific tools such as SVM and clustering are used to perform the optimization and propagate uncertainty.

The next steps of this research will increase the dimensionality of the problem and apply the proposed methodology to other types of NES, including the important "ungrounded" configuration.

6 ACKNOWLEDGMENTS

The support of the National Science Foundation (grant CMMI-1029257) is gratefully acknowledged.

REFERENCES

[1] Gendelman, O., Manevitch, L., Vakakis, A. F., and M'closkey, R., 2001. "Energy pumping in nonlinear mechanical oscillators: Part i: Dynamics of the underlying hamiltonian systems". *Journal of Applied Mechanics,* ***68***(1), pp. 34–41.

[2] Vakakis, A. F., Kounadis, A. N., and Raftoyiannis, I. G., 1999. "Use of non-linear localization for isolating structures from earthquake-induced motions". *Earthquake engineering & structural dynamics,* ***28***(1), pp. 21–36.

[3] Wierschem, N., Spencer Jr, B., Bergman, L., and Vakakis, A., 2011. "Numerical study of nonlinear energy sinks for seismic response reduction". In Proceedings of the 6 th International Workshop on Advanced Smart Materials and Smart Structures Technology (ANCRiSST 2011), pp. 25–26.

[4] Lee, Y. S., Vakakis, A. F., Bergman, L. A., McFarland, D. M., and Kerschen, G., 2008. "Enhancing the robustness of aeroelastic instability suppression using multi-degree-of-freedom nonlinear energy sinks". *AIAA journal,* ***46***(6), pp. 1371–1394.

[5] Gourdon, E., and Lamarque, C.-H., 2006. "Nonlinear energy sink with uncertain parameters". *Journal of computational and nonlinear dynamics,* ***1***(3), pp. 187–195.

[6] Gendelman, O., and Bergman, L., 2008. *Nonlinear targeted energy transfer in mechanical and structural systems*, Vol. 156. Springer.

[7] Hartigan, J.A., and Wong, M.A., 1979. "A k-means clustering algorithm". *Applied Statistics,* ***28***, pp. 100–108.

[8] Basudhar, A., and Missoum, S., 2010. "An improved adaptive sampling scheme for the construction of explicit boundaries". *Structural and Multidisciplinary Optimization*, pp. 1–13.

[9] Basudhar, A., and Missoum, S., 2009. "A sampling-based approach for probabilistic design with random fields". *Computer Methods in Applied Mechanics and Engineering,* ***198***(47-48), pp. 3647 – 3655.

[10] Gunn, S.R., 1998. Support vector machines for classification and regression. Tech. Rep. ISIS-1-98, Department of Electronics and Computer Science, University of Southampton.

[11] Cristianini, N., and Schlkopf, B., 2002. "Support vector machines and kernel methods: The new generation of learning machines". *Artificial Intelligence Magazine,* ***23***(3), pp. 31–41.

[12] Missoum, S., Dribusch, C., and Beran, P., 2010. "Reliability-based design optimization of nonlinear aeroelasticity problems". *Journal of Aircraft,* ***47***(3), pp. 992–998.

[13] Santner, T., Williams, B., and Notz, W., 2003. *The design and analysis of computer experiments*. Springer Verlag.

[14] Sacks, J., Welch, W. J., Mitchell, T. J., and Wynn, H. P., Nov., 1989. "Design and analysis of computer experiments". *Statistical Science,* ***4***(4), pp. 409–423.

[15] Melchers, R., 1999. *Structural Reliability Analysis and Prediction*. John Wiley & Sons.